D422Lot1.SMHI.5.1.1B: Detailed workflows of each case-study on how to use the CDS for CII production and climate adaptation Full Technical Report: Climate change effects on major d...

Technical Report · February 2019

DOI: 10.13140/RG.2.2.22041.57447

2 authors:


Remegio B. Confesor
Norwegian Institute of Bioeconomy Research


Tian Guo
Purdue University

D422Lot1.SMHI.5.1.1B:

Detailed workflows of each case-study on how to use the CDS for CII production and climate adaptation

Full Technical Report:

Climate change effects on major drivers of harmful algal blooms (HABs): best management practices and HAB severity

Remegio Confesor Jr., Ph.D.

Tian Guo, Ph.D.

National Center for Water Quality Research, Heidelberg University, Ohio, USA

REF.: C3S_422_Lot1_SMHI D5.1.1B

Summary

This technical report documents the description and findings of the case study entitled "Climate change effects on major drivers of HABs in Lake Erie in the United States" implemented by the National Center for Water Quality Research (NCWQR), Heidelberg University, Ohio, USA. This report is divided into five main sections: 1) description of the case study, 2) potential adaptation measures, 3) contact, 4) data production and results, and 5) conclusions.

The Copernicus Climate Change Service (C3S) platform provided downscaled and bias-corrected climate indicators in which the locally-produced climate indicators in the Western Lake Erie Basin can be compared and verified with. The platform also provided an easy access to climate indicators and essential climate variables (ECV's) that could be used to develop and test other mitigation approaches.

The results showed that increased temperature and precipitation would increase the annual occurrence of severe algal blooms to 24% in the 2050's. However, the implementation of best management practices (BMPs) could reduce this risk down to 12%, similar to the past 16 years.

Currently recommended mitigation approaches on top of the existing practices are enough to maintain the risk level of severe algal blooms occurrence even with climate change effects in the future. However, "out-of-the-box" mitigations are necessary to further lower the risks of severe algal bloom occurrence than the current levels.

Contents

1-Case study description

1.1 Issue to be addressed

The recurrence of harmful algal blooms (HABs) in the Western Lake Erie Basin (WLEB) is mainly attributed to the increase in soluble reactive phosphorus (SRP) loads to Lake Erie. The extent of the HABs in the summer of 2011 and 2015 was also the largest in the last decade. There is a consensus among the researchers, government agencies, and stakeholders that this increase in SRP is mainly coming from the agricultural lands of the Lake Erie watersheds. While current efforts are geared toward achieving the 40% nutrient reduction set by the 2012 Great Lakes Water Quality Agreement (GLWQA) between the United States and Canada, the effects of climate change on these reduction strategies have not been fully understood. Thus, this case study quantified the amount of nutrient exports and the corresponding algal bloom severity under different future climate scenarios and mitigation practices. The results will help inform and prepare better the stakeholders (e.g., farmers, government agencies (local, state, federal), policymakers, and non-governmental organizations (NGOs)) against the effects of climate change.

1.2 Decision support to client

We provided and discussed the results of the project with the client, the Toledo Metropolitan Area Council of Governments (TMACOG), composed mainly of government agencies, private entities, and NGOs in northwest Ohio and southeast Michigan. We envisioned that these stakeholders will use these results to develop contingency management plans in anticipation of the climate change effects on water quality and quantity at Lake Erie. Specifically, this project tested effective practices that the client could implement to reduce nutrient exports (hence, HABs) regardless of the climate change effects.

1.3 Temporal and spatial scale

The average of twenty-year baseline and future projections (2002-2017, 2040-2060) of the selected CIIs were provided and discussed with the client and stakeholders. This case study focused on the Maumee watershed, a major load contributor to Lake Erie. Management and mitigation practices were usually implemented at the field (~10 hectares) to watershed level (>90 km^2).

1.4 Knowledge brokering

We have presented the objectives of this project to the client and asked for their ranking of the CIIs according to their needs (Table 1). We also presented the results of this study in October, 2018. The clients were excited and amazed on the results of the study (e.g., the CIIs and water quality impacts) and discussed how this informed them about the effects of climate change. They were quite appreciative of the Copernicus Climate Change Service (C3S) platform where they could interactively explore the climate change effects in their local area.

Table 1. Climate Impact Indicators (CII) for the Western Lake Erie Basin project.

Climate Impact Indicator (CII)	Unit	From Essential Climate Variable
Air temperature, e.g. annual, monthly or daily max. min., mean	°C	Air temperature at 2 m
Degree days for heating and cooling, respectively; outdoor vs indoor temp.	°C	Air temperature at 2 m
Drought; agricultural and hydrological, respectively, below threshold	days	Soil moisture and river flow, respectively
Growing season; leaf on/off, season length, Growing/senescence days	Date, days, °C days	Air temperature at 2 m and local/regional thresholds
Heat wave duration and No. hot days	days, °C* days	Air temperature at 2 m and percentile thresholds
Ice days; daily max. temp. less than 0°C	days	Air temperature at 2 m
Frost days; daily min. temperature less than 0°C.	days	Air temperature at 2 m
Floods; return periods of high flows	years	Daily river flow and local/regional thresholds
Precipitation e.g. annual, monthly or daily max. min., mean	mm	Precipitation
Short-duration extreme precipitation	mm/hr	Precipitation
Surface-water temperature	°C	Daily temperature in river flow
Soil Temperature; monthly average	°C	Daily temperature at 10 cm depth
Snow cover and water equivalent	days, mm	Snow storage above 1 cm
Snow water equivalent	mm	Daily snow storage
Water runoff or discharge, e.g. annual, monthly or daily: max., min., mean	mm, m^3/s	Daily surface flow
Nutrient and sediment exports	tons	From impact models
Algal Bloom Extent	km^2	From impact models

2-Potential adaptation measures

2.1 Lessons learnt

With the current climate conditions, “there is no silver bullet” solution in reducing the magnitude and intensity of harmful algal blooms. Past and current multi-modeling projects at the watershed scale reduced the uncertainty of impact models and pointed to the right practices of reducing nutrients and sediments that feed the algal blooms. We have experienced that a multi-sectoral and interdisciplinary collaboration will lead to a science-based viable solutions and consensus in reducing the algal blooms. Lastly, we learned that stakeholder consultations and inputs are necessary in impact modeling projects.

2.2 Importance and relevance of adaptation

Current management practices and load reduction efforts do not account for the effects of climate change and the export reduction effectiveness of these practices in future climate is unknown. Adaptation includes identifying and implementing practices that would reduce nutrient and sediment loading (hence, algal blooms) regardless of the changing climate. Thus, climate adaptation would direct current resources and efforts to explore mitigation efforts that would reduce efficiently future algal bloom occurrence despite climate change effects.

2.3 Pros and cons or cost-benefit analysis of climate adaptation

There have been tremendous economic losses due to algal blooms in Lake Erie. The defining moment was when regulators banned Toledo's tap for drinking and cooking for two days in early August 2014 when the water was found contaminated with toxins from Microcystis cyanobacteria bloom. It cannot be emphasized enough that the risks of such drastic conditions to occur again increases without climate mitigation and adaption. Researchers have started to analyze the benefits and cost of implementing management practices but without considering the effects of climate change and mostly at the agricultural farm level. We advocate an integrated cost-benefit analyses that would encompass the costs, profit margins, and environmental outputs from all sectors (e.g., farmers, fishermen, boaters, resorts, etc.) in the western basin of Lake Erie and its watersheds.

2.4 Policy aspects

As has been discussed earlier, the annex 4 of the Great Lakes Water Quality Agreement (GLWQA) between the USA and Canada calls for a 40% reduction of phosphorus loads from the 2008 level. Domestic action plans are currently being developed at the federal and state levels to reduce phosphorus exports to Lake Erie. The information derived from this contract would certainly help in the adaptive management approach in phosphorus reduction and of the algal bloom problem in general.

3-Contact

3.1 Purveyors

Rem Confesor Jr., Ph.D., National Center for Water Quality Research (NCWQR), Heidelberg University, Tiffin, USA

3.2 Clients/users

Tim Murphy, Toledo Metropolitan Area Council of Governments (TMACOG) Watersheds Committee, Toledo, USA

4- Data production and results

The project workflow (Figure 1) is composed of five steps (explained in detail below): 1) data acquisition and processing, 2) impact model setup, 3) production of local CIIs, 4) algal bloom extent estimation, and 5) impact assessment and dissemination. Except for Step 2, the succeeding steps are dependent from the previous stages of the workflow. The workflow facilitated effective execution of specific tasks and accomplishment of the objectives in each project phase. Quality assurance and quality control (QA/QC) were implemented in each step before proceeding to the next phase of the project. Thus, the overall goal and deliverables of the project were achieved using the workflow.

Figure 1. Project Workflow.

4.1 Step 1: Data download and processing.

Description:

STEP 1.a. Data acquisition. Historical and RCP 8.5 data of 19 GCM ensembles (Table 2), downloadable from the climate data store (CDS) catalogue were used for downscaling and bias-correction. Climate variables were the daily precipitation, maximum temperature, and minimum temperature data for these 19 GCMs from 1981-2005 (historical period) (see Step 1b below). The GCM data from 2006 to 2100 were also downscaled to 20x20 km grid resolution (see Step1b) and bias-corrected using the DBS method (Yang et al., 2010). Bias-corrected data (0.5° grid resolution) for historical and RCP 8.5 scenarios were also downloaded from the C3S contract and used to verify the locally produced CIIs (see section 4.3, Step 3). The study area, Maumee watershed, is within 82.50 W to 86.00 W longitudes and from 40.50 N to 42.25 N in latitudes.

Table 2. Global Circulation Models (GCMs) used in this case study.

Institute	Model	GCMName	GCMCode	Remarks
BCC	CSM1-1	bcc-csm1-1	BCCSM1	Beijing Climate Center
BNU	ESM	BNU-ESM	BNUESM	Beijing Normal University
CNRM	CNRM-CM5	CNRM-CM5	CNRCM5	National Centre for Meteorological Research, France
CSIRO-QCCCE	CSIRO-Mk3-6-0	CSIRO-Mk3-6-0	CSI360	Commonwealth Scientific and Industrial Research Organization/ Queensland Climate Change Centre of Excellence (CSIRO-QCCCE)
CSIRO-BOM	ACCESS1-0	ACCESS1-0	CSIS10	Centre for Australian Weather and Climate Research (CAWCR)
CSIRO-BOM	ACCESS1-3	ACCESS1-3	CSIS13	Centre for Australian Weather and Climate Research (CAWCR)

SMHI	EC-EARTH	EC-EARTH	EEARTH	A European community Earth-System Model, led by SMHI, Sweden
GFDL	CM3	GFDL-CM3	GFDCM3	Geophysical Fluid Dynamics Laboratory, NOAA
GFDL	ESM2G	GFDL-ESM2G	GFDM2G	Geophysical Fluid Dynamics Laboratory, NOAA
GFDL	ESM2M	GFDL-ESM2M	GFDM2M	Geophysical Fluid Dynamics Laboratory, NOAA
MOHC	HadGEM2-CC	HadGEM2-CC	HAD2CC	Met Office Hadley Centre, Hadley Global Environment Model, UK
MOHC	HadGEM2-ES	HadGEM2-ES	HAD2ES	Met Office Hadley Centre, Hadley Global Environment Model, UK
INM	CM4	INMCM4	INMCM4	Russian Institute for Numerical Mathematics Climate Model Version 4
IPSL	CM5A-LR	IPSL-CM5A-LR	IPSALR	Institut Pierre Simon Laplace, France
IPSL	CM5A-MR	IPSL-CM5A-MR	IPSAMR	Institut Pierre Simon Laplace, France
IPSL	IPSL-CM5B-LR	IPSL-CM5B-LR	IPSBLR	Institut Pierre Simon Laplace, France
MPI	ESM-LR	MPI-ESM-LR	MPIMLR	Max Planck Institute, Germany
MPI	MPI-ESM-MR	MPI-ESM-MR	MPIMMR	Max Planck Institute, Germany
NCC	NorESM1-M	NorESM1-M	NORM1M	Norwegian Climate Centre Earth System Model M

Step 1.b. Spatial downscaling method was used in this study to calculate fine-scale information based on coarse-scale information using the spatial interpolation method (Flint and Flint, 2012). The spatial downscaling for the 19 GCMs were performed to daily precipitation, maximum temperature and minimum temperature data from PRISM dataset with the 4-km grid resolution from 1981 to 2005 (Flint and Flint, 2012). The PRISM dataset is a widely used analytical model integrating point data of measured precipitation and temperature (Daly et al., 1994).

The downscaled daily precipitation, maximum temperature, and minimum temperature data for the 19 GCMs were then bias-corrected. The transfer functions were derived using natural cubic regression splines based on the historical (1981-2005) daily observed vs. simulated weather data and then applied to the future scenario (2006-2100). The sequence of interior knots for each dataset from each GCM were adjusted to determine the smoothest possible curve to fit the observed data. We assume that the functions are strictly monotonic and obtained the inverse functions (GCM historical as the independent (x) variable and both the PRISM observed and the GCM future scenarios as the dependent (y) variable). Since both the PRISM and GCM data were sorted from lowest to highest value, the derived equations were monotonic functions and the assumption was valid.

Step 1.c. We also utilized the existing DEM, soils, land use, observed weather data, management practices data and process for input to local (Maumee) HYPE model. These data were previously acquired for SWAT setup.

Results:

We tested different downscaling resolutions (Figure 2) and results showed that the 20x20 km resolution yielded comparable impact model (Soil and Water Assessment Tool, SWAT) simulations with the 4x4 km and 16x16 grid resolutions (see Figures 3 and 4) but considerably took less processing time. Thus, the 20x20 km grid resolution was used for the downscaling and bias-correction.

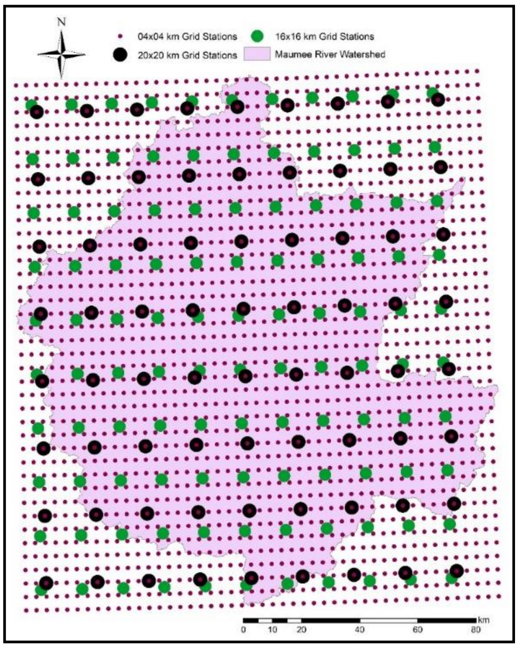

Figure 2. Station resolutions used in downscaling and bias-correction.

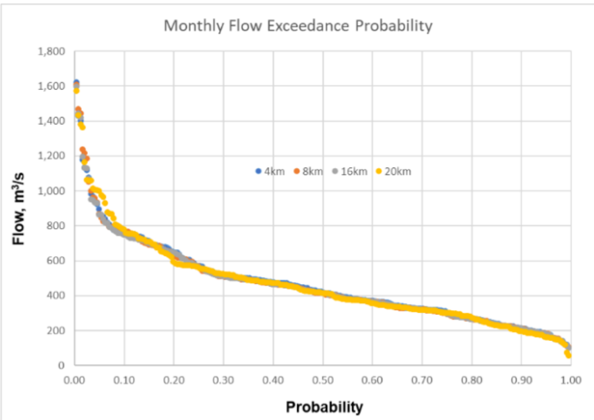

Figure 3. SWAT-derived flow exceedance probability run at different weather station resolutions.

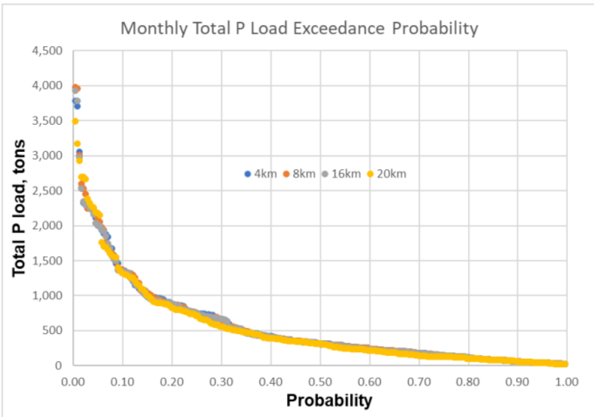

Figure 4. SWAT-derived total P load exceedance probability run at different weather station resolutions.

Step 1.d. ECV verification.

Description:

To verify the locally produced data, we compared the bias-corrected ECV data from the C3S contract at one station (N41.750000, W85.250000) with the nearest local downscale station (N41.729167, W85.229167).

Results:

The probability distribution for the bias-corrected precipitation, maximum temperature and minimum temperature in this case study matched well with those data from the C3S during historical (1981 to 2005) and future (2031 to 2055) periods for three randomly selected GCMs (ACCESS1-0, CNRM-CM5 and GFDL-ESM2M) (Figures 5-7).

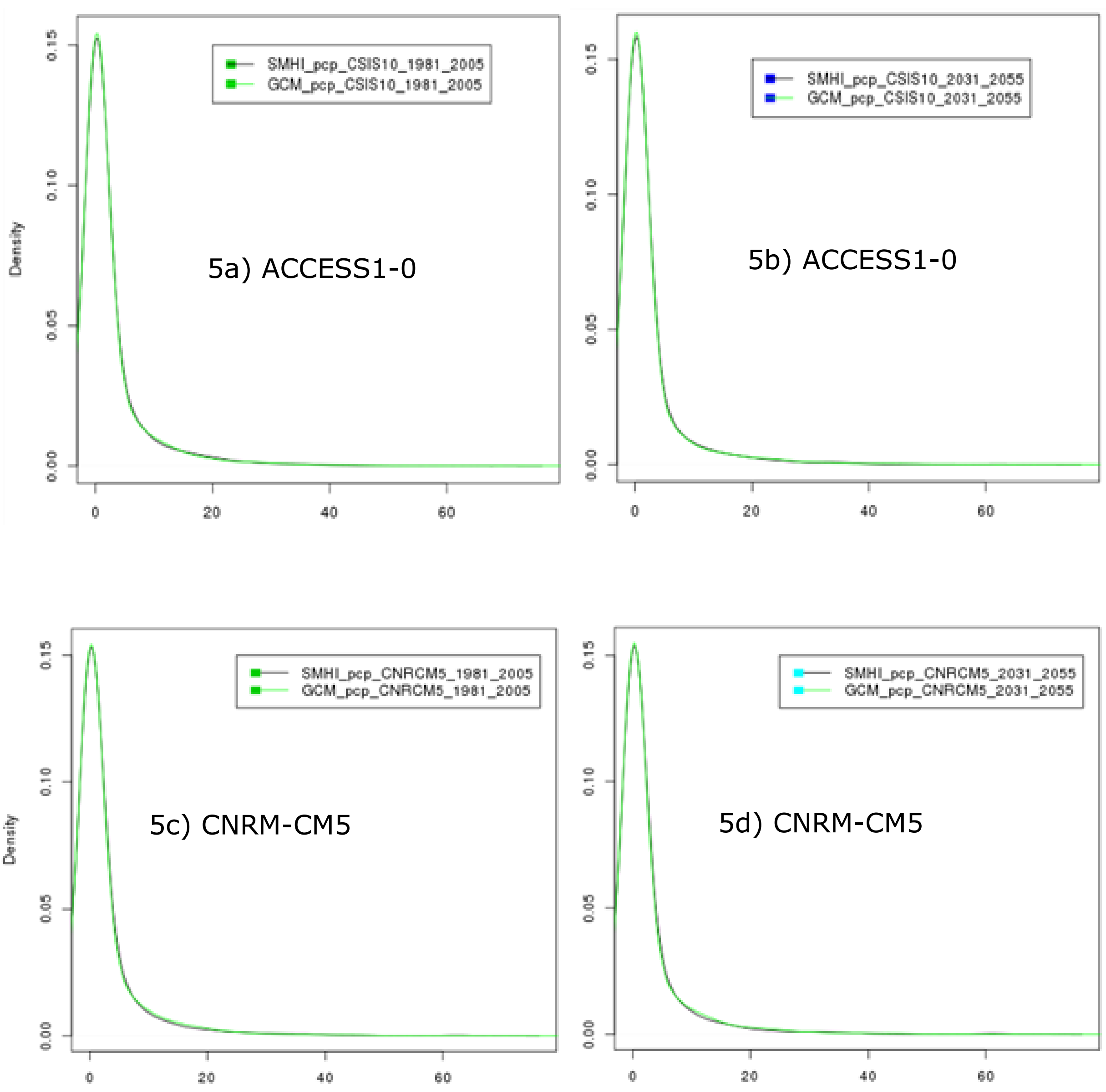

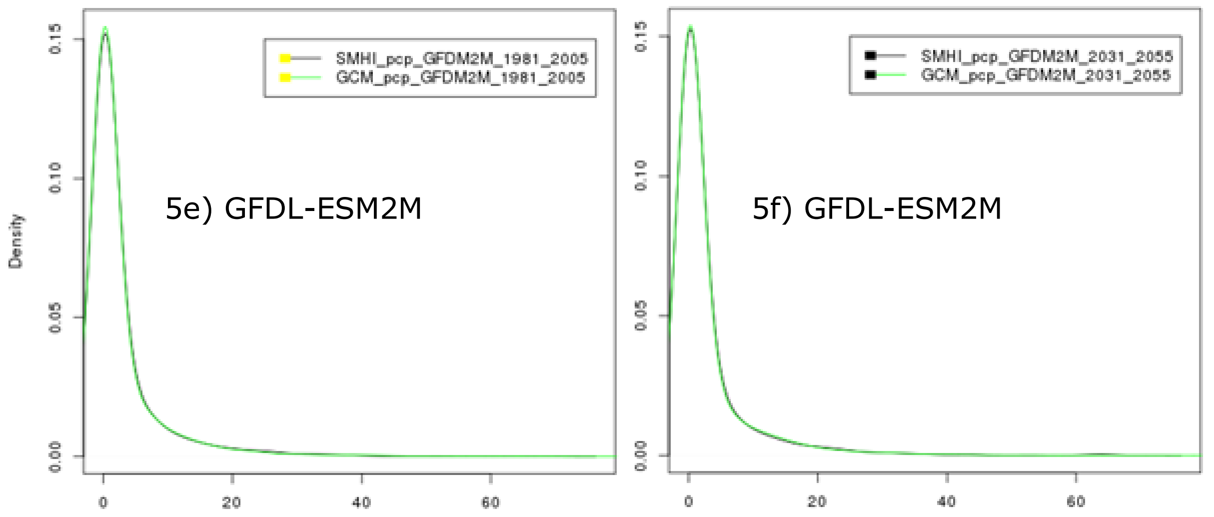

Figure 5. The probability distribution of the bias-corrected precipitation in this case study and the Copernicus Climate Change Service for the three selected GCMs (ACCESS1-0, CNRM-CM5 and GFDL-ESM2M) during historical (1981 to 2005) (a, c and e) and future (2031 to 2055) (b, d and f) periods.

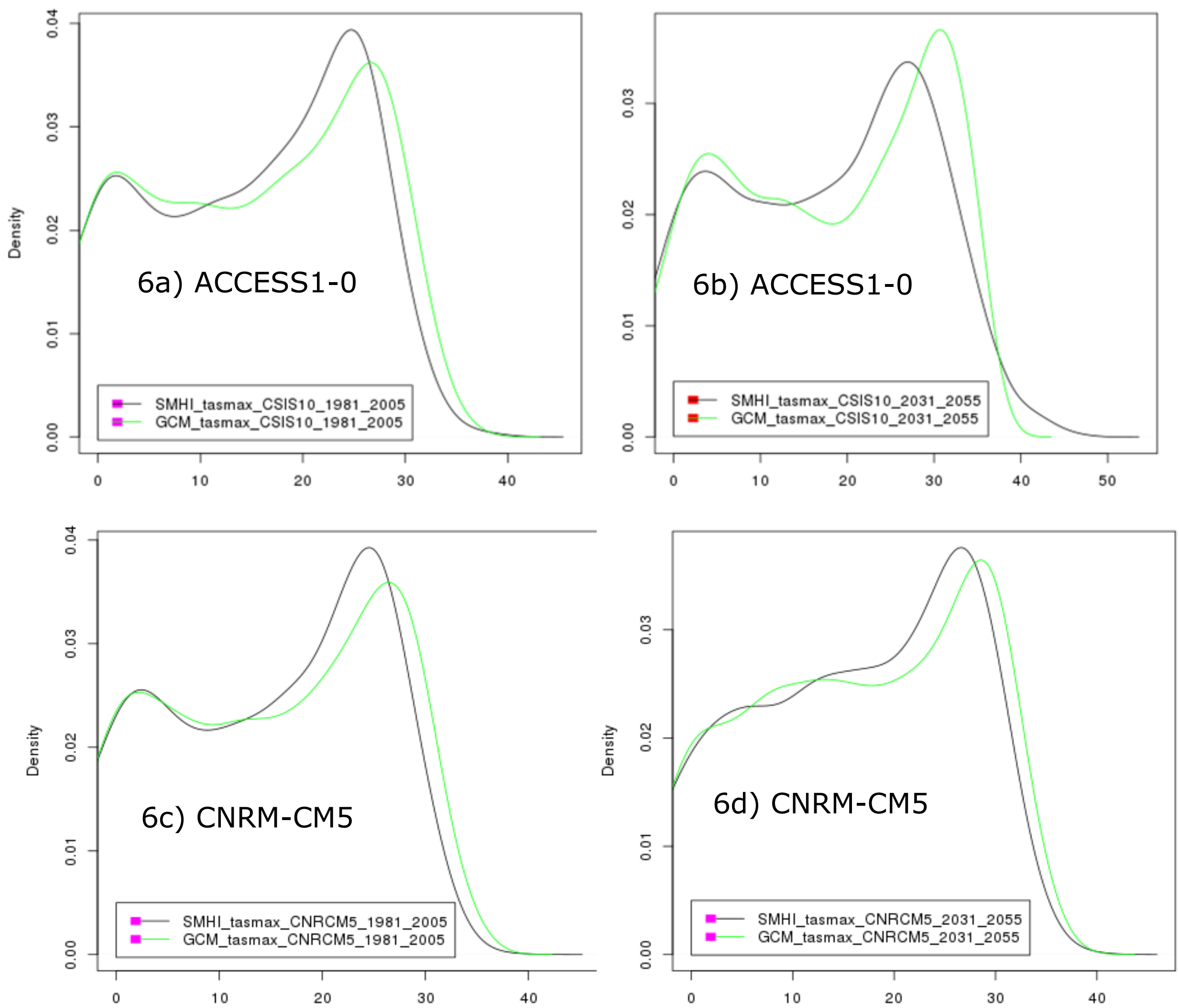

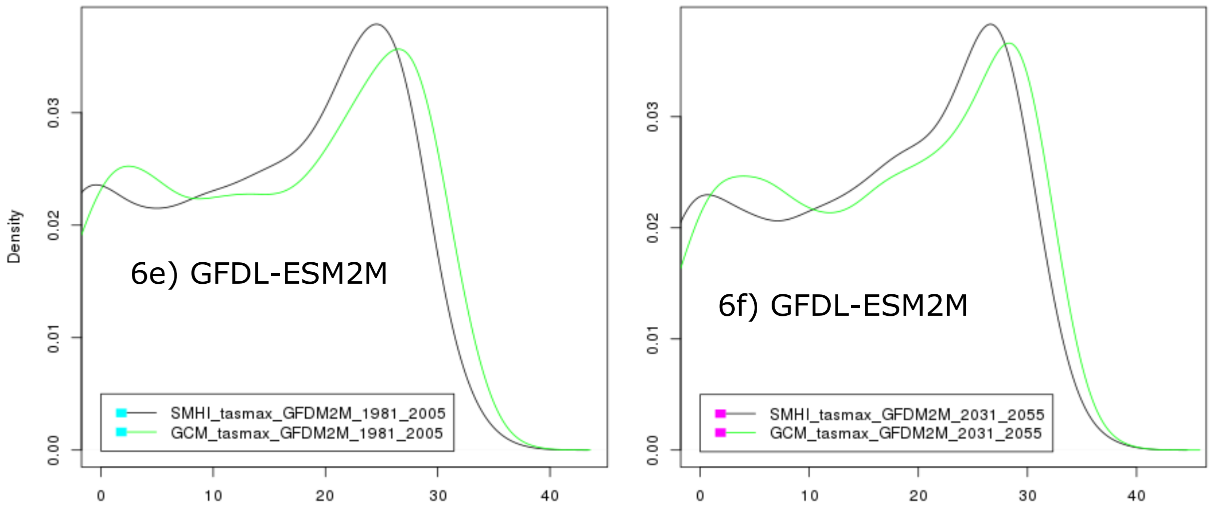

Figure 6. The probability distribution of the bias-corrected maximum temperature in this case study and the Copernicus Climate Change Service for the three selected GCMs (ACCESS1-0, CNRM-CM5 and GFDL-ESM2M) during historical (1981 to 2005) (a, c and e) and future (2031 to 2055) (b, d and f) periods.

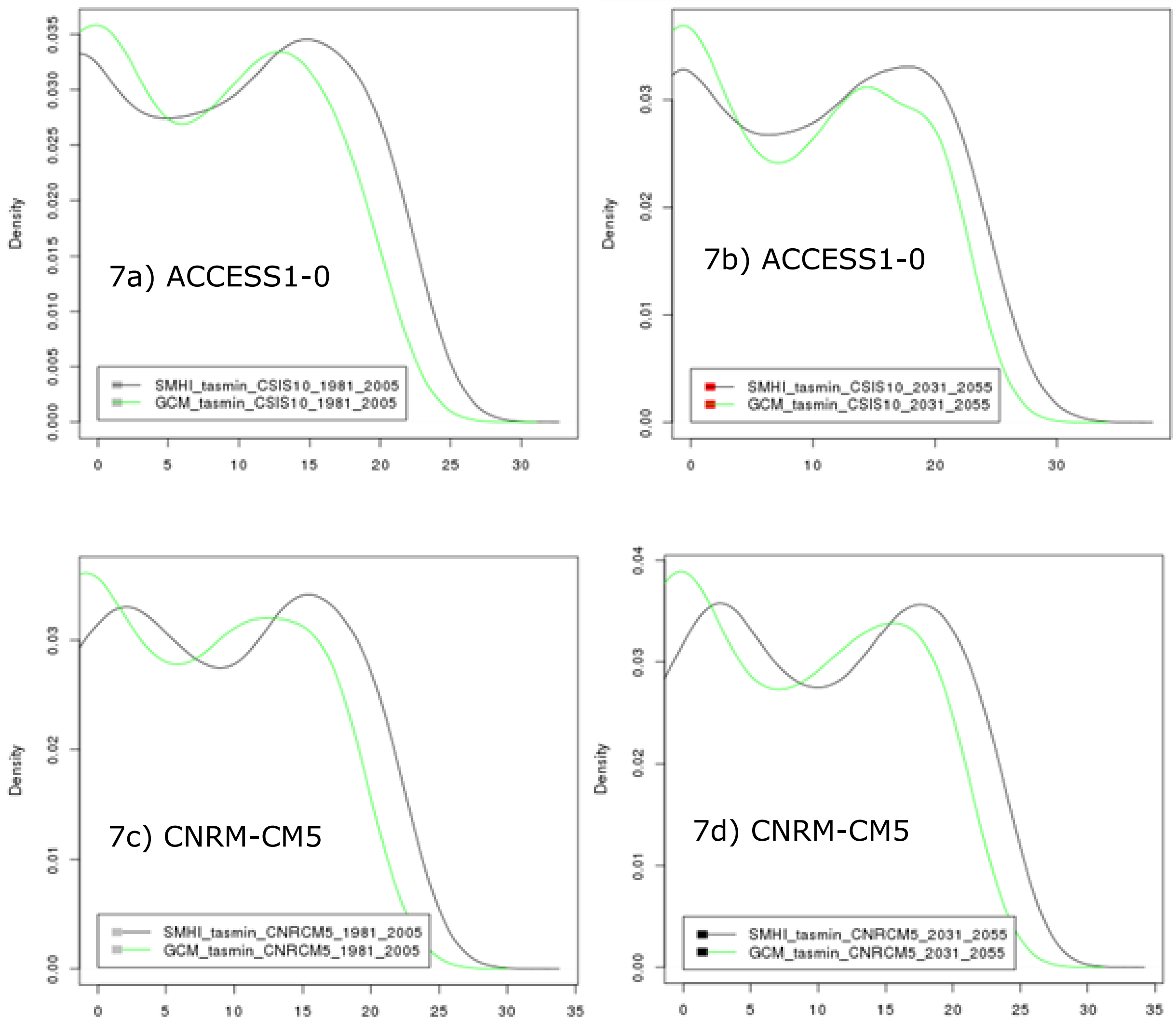

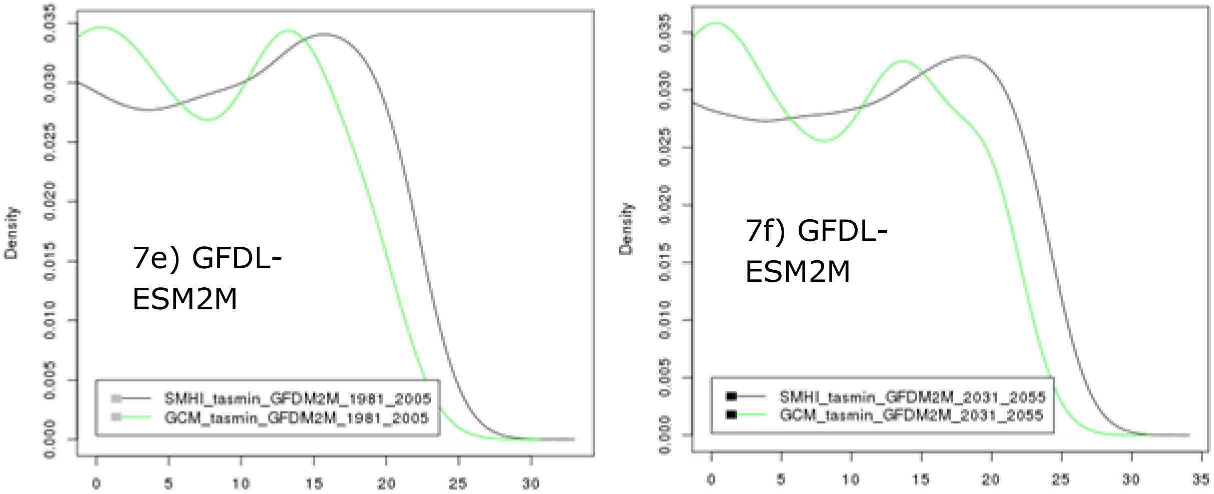

Figure 7. The probability distribution of the bias-corrected minimum temperature in this case study and the Copernicus Climate Change Service for the three selected GCMs (ACCESS1-0, CNRM-CM5 and GFDL-ESM2M) during historical (1981 to 2005) (a, c and e) and future (2031 to 2055) (b, d and f) periods.

The variables derived directly from the downscaling, bias correction, and analysis of GCM data (e.g., daily, monthly, annual, decadal, and 20-year) precipitation, minimum temperature, and maximum temperature, etc.) are used as the main forcing inputs to the SWAT impact model.

The 20-yr average annual precipitation show an increasing trend from the 1980’s to the 2100 with the changing climate (Figure 8).

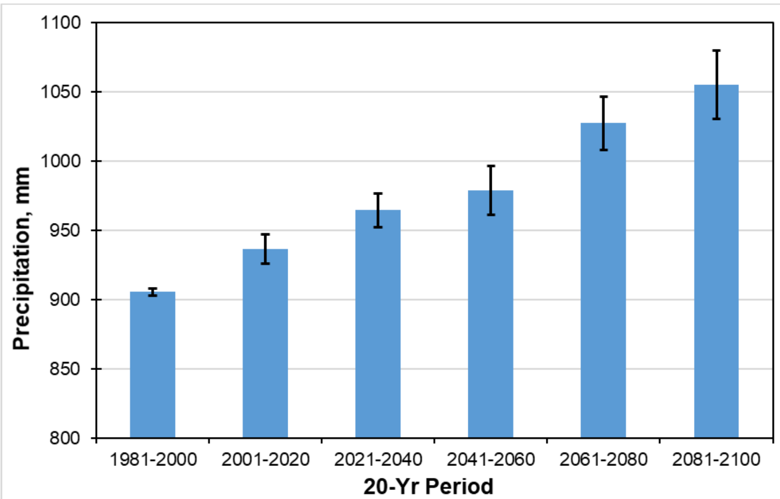

Figure 8. Increasing precipitation trend from 1981 to 2100.

4.2 Step 2: Hydrological models setup.

Description:

The SWAT model was previously calibrated and validated using the methods described in Scavia et al., 2017. The HYPE hydrological catchment model was set up to simulate the streamflow at the USGS Blanchard River (USGS 04189000), Tiffin River (USGS 04185000) and Maumee River (USGS 04193500) stations in Ohio, USA. HYPE model inputs were prepared based on model inputs used in the SWAT model in Maumee watershed in the previous projects. The soil, slope, land use, rotation data, the combinations of soil and land use (SLCs), crop management practices, and point source pollution data were derived from those developed in the SWAT. The representation of sub-basin characteristics, subsurface drainage systems and weather data in the HYPE were as same as those were used in the SWAT. The soil data from SSURGO in the SWAT were classified as nine soil types in the HYPE based on soil water holding capacity. The 13 major land use types in the SWAT were classified as eight land use types in the HYPE. The 142 SLCs representing the combinations of land use, soil, rotations were reclassified and the percentage of the area of each subbasin as the area for each SLC were calculated and then incorporated in Geodata.

Daily streamflow between Jan 1, 2010 and Dec 31, 2015 at USGS Blanchard, Tiffin and Maumee River stations were used for HYPE model calibration with the warm-up period between Jan 1, 2000 and Dec 31, 2009. The hydrological processes-related parameters, wcep (effective porosity as a fraction), rivvel (Celerity of flood in watercourse, m/s)), cevp (Potential evapotranspiration rate, mm/day/℃)), rrcs1 (Soil runoff coefficient for the uppermost soil layer, /day), cevpcorr (Correction factor for evapotranspiration), and rivvel2 (parameter for calculation of velocity of the water in the watercourse) were calibrated manually (Yin et al., 2016). Hydrographs and statistical criterions, Percent error (PBIAS), Nash-Sutcliffe coefficient (NSE), coefficient of determination (R2), and root mean squared error (RMSE) were used to evaluate model performance in simulating daily water discharge (Yin et al., 2016).

Results:

The calibrated SWAT model could accurately simulate daily streamflow discharge, and sediment, TP, SRP, TN, and NO3 loads from 2005 to 2015 at the Maumee River station in Waterville, OH (Scavia et al., 2017). The calibrated HYPE model could accurately simulate daily streamflow discharge from 2010 to 2015 at Blanchard, Tiffin and Maumee River stations. Due to time constraints in further verifying the HYPE simulations, the results only from SWAT were used and presented in this report.

4.3 Steps 3: Production of local CIIs.

Description:

The local CIIs include the simulated stream discharge, nutrients (N and P), and sediment exports by the SWAT impact model with the GCM forcing input.

Results:

The spreads of the annual means for flow discharge, total flow volume, and sediment, total nitrogen (TN), total phosphorus (TP), soluble reactive phosphorus (SRP) and nitrate (NO3) loads (Figure 9), and means during spring for flow volume, TP, and SRP loads (Figure 10) from 1998 to 2017 of the 19 GCMs simulated at 20x20 km grid resolution were similar to those of the data from the SWAT calibrated model using PRISM weather data at 4x4 km grid resolution. The Cumulative density graphs and probability density graphs of the monthly average flow discharge, and sediment, TN, TP, SRP and NO3 loads for the simulated data 1998 and 2017 were similar to those of the PRISM calibrated simulation as well (Figure 11).

The spreads of the simulated spring total flow volume, and TP and SRP loads from the 19 GCMs were similar to each other in the periods 2041-2060 (Figure 12) and 2081-2100 (Figure 13).

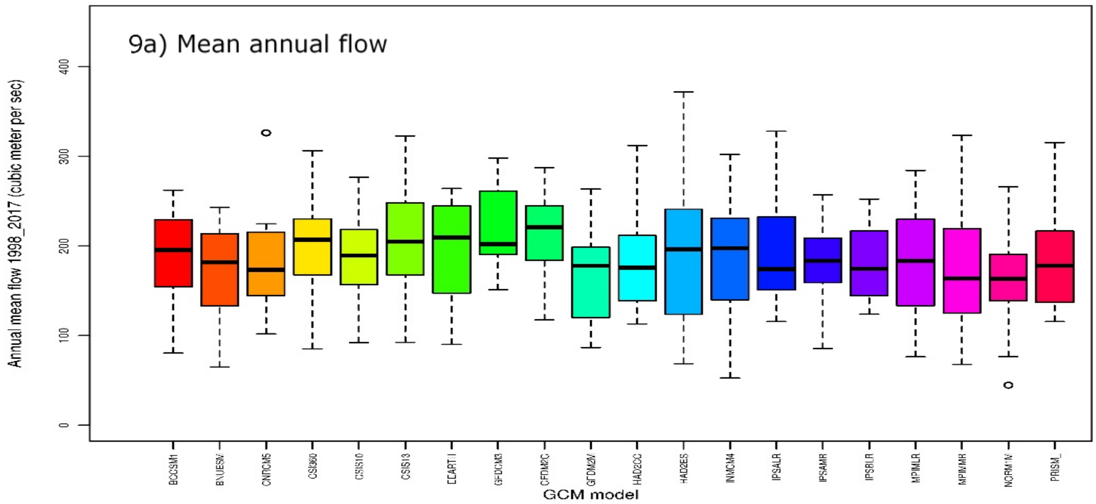

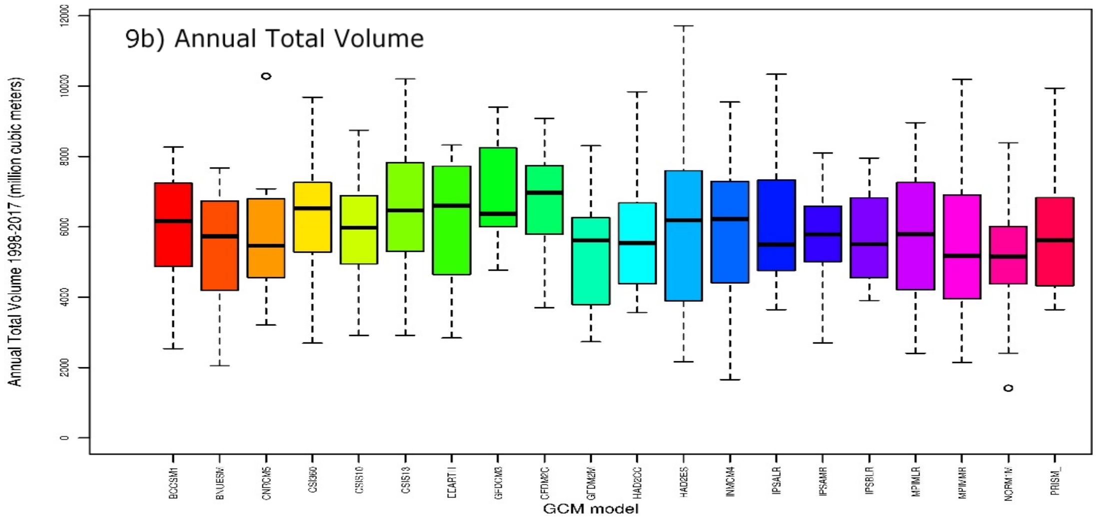
9b) Annual Total Volume
Annual Total Volume 1998-2017 (million cubic meters)
GCM model

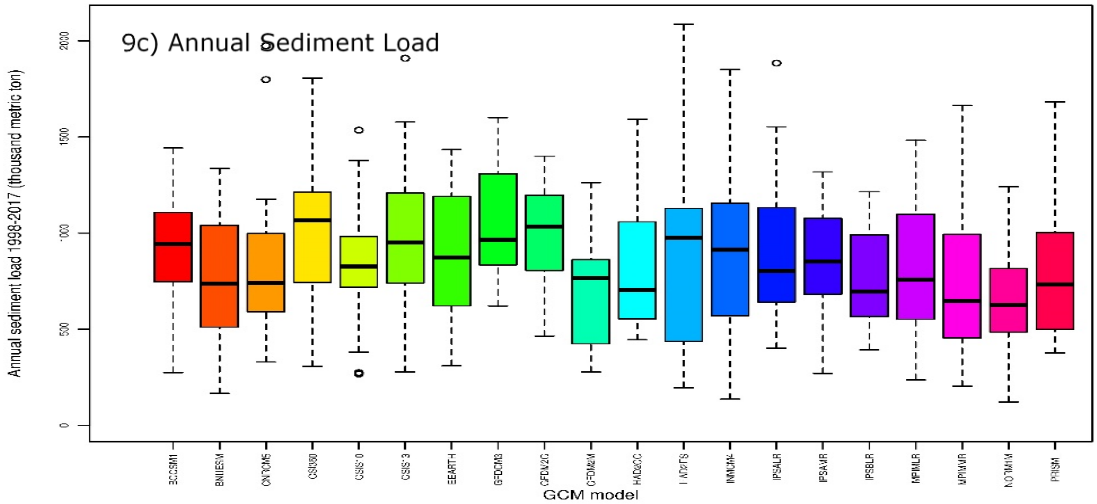
9c) Annual Sediment Load
Annual sediment load 1998-2017 (thousand metric ton)
GCM model

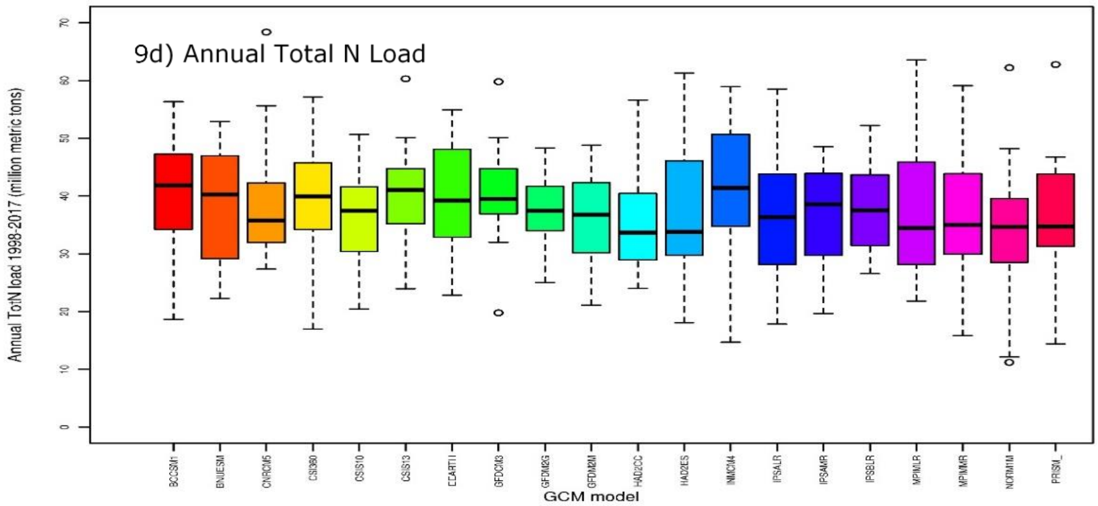
9d) Annual Total N Load
Annual TotN load 1998-2017 (million metric tons)
GCM model

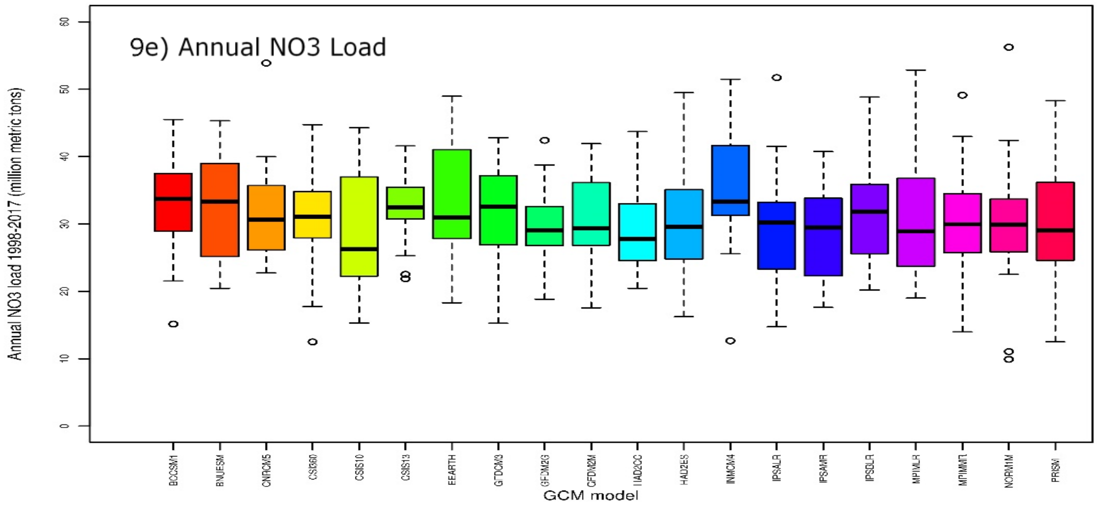

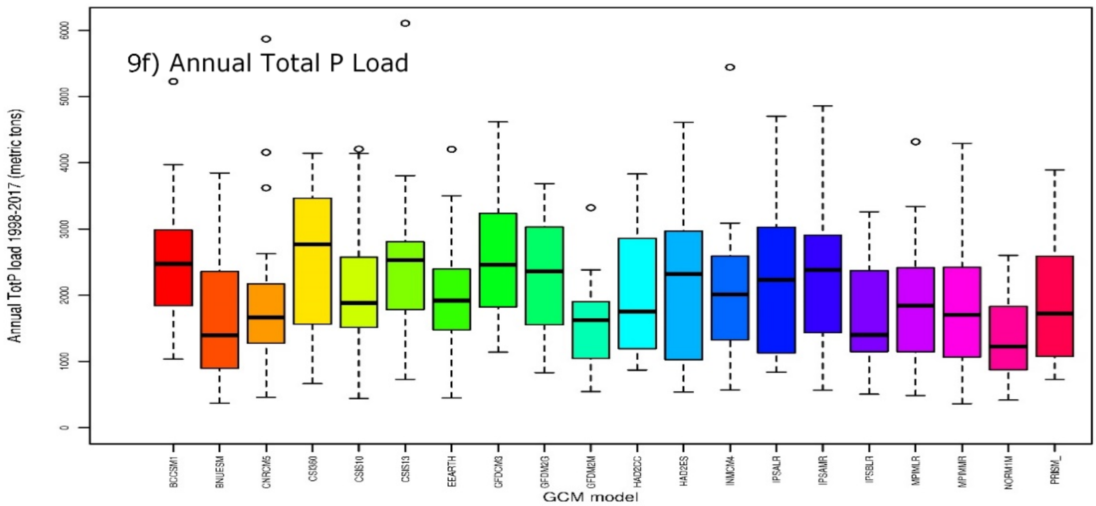

Figure 9. Boxplots of annual mean flow discharge (a), total flow volume (b), and sediment (c), total nitrogen (TN) (d), total phosphorus (TP) (e), soluble reactive phosphorus (SRP) (f) and nitrate (NO_3) (g) loads for the 19 GCMs and PRISM data simulated with SWAT for the USGS Waterville station (N41.5000, W83.7128) from 1998 to 2017.

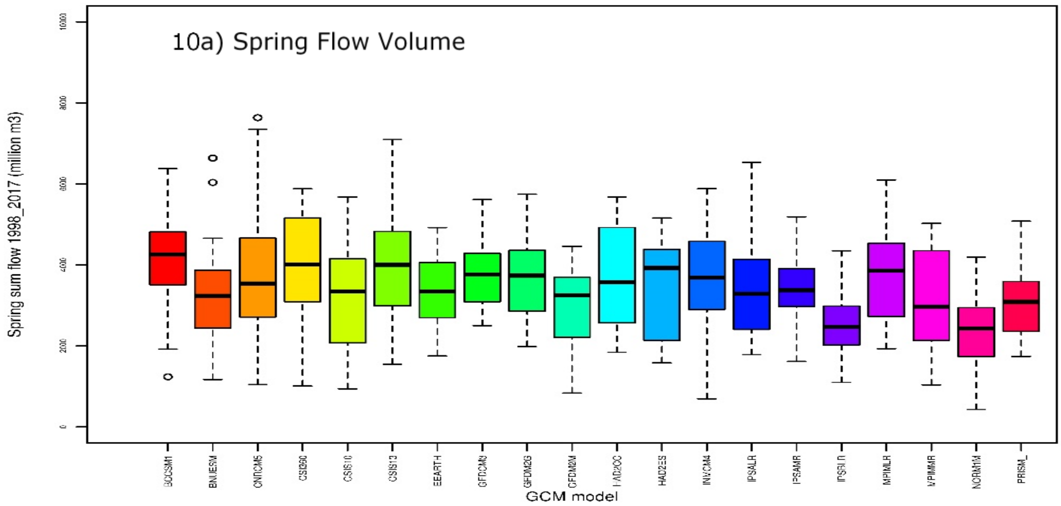

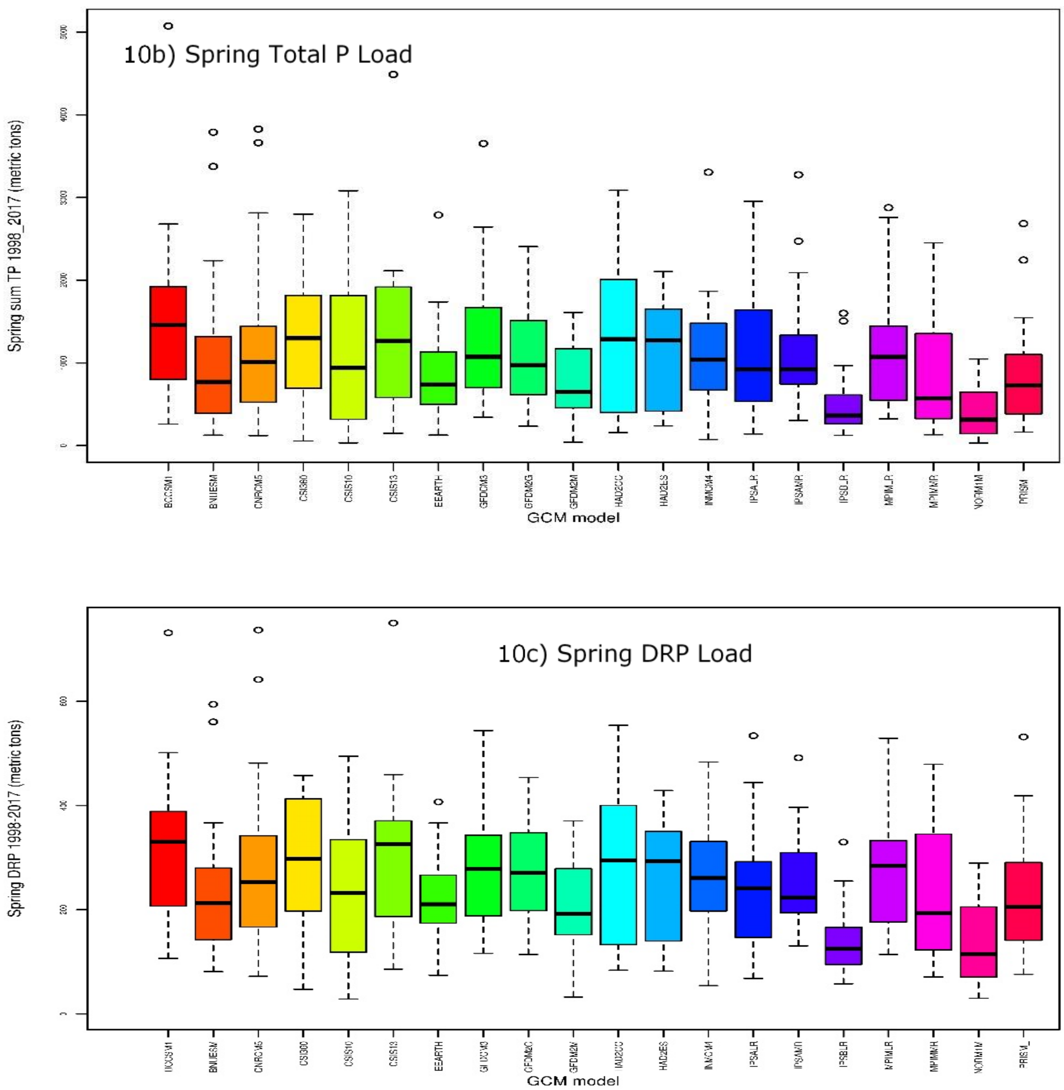

Figure 10. Boxplots of a) spring total flow volume, b) Total P load, and c) SRP load for the 19 GCMs and PRISM data simulated with SWAT for the USGS Waterville station (N41.5000, W83.7128) from 1998 to 2017.

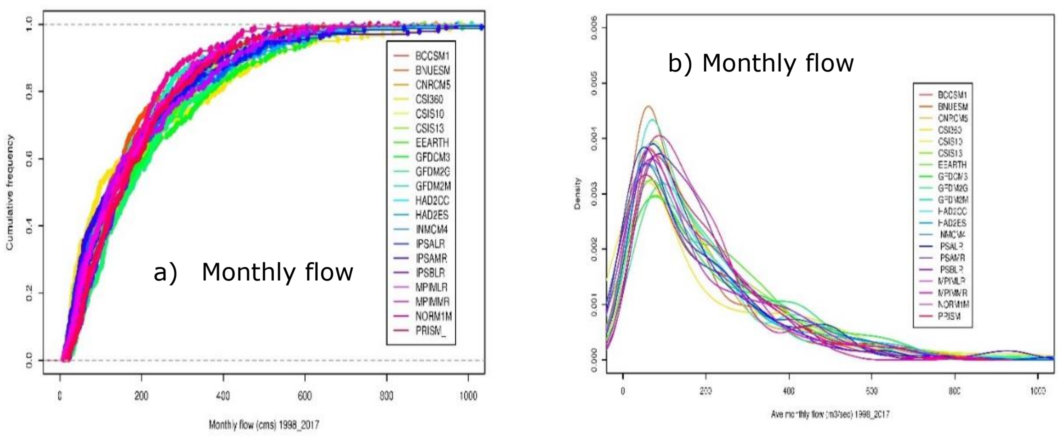

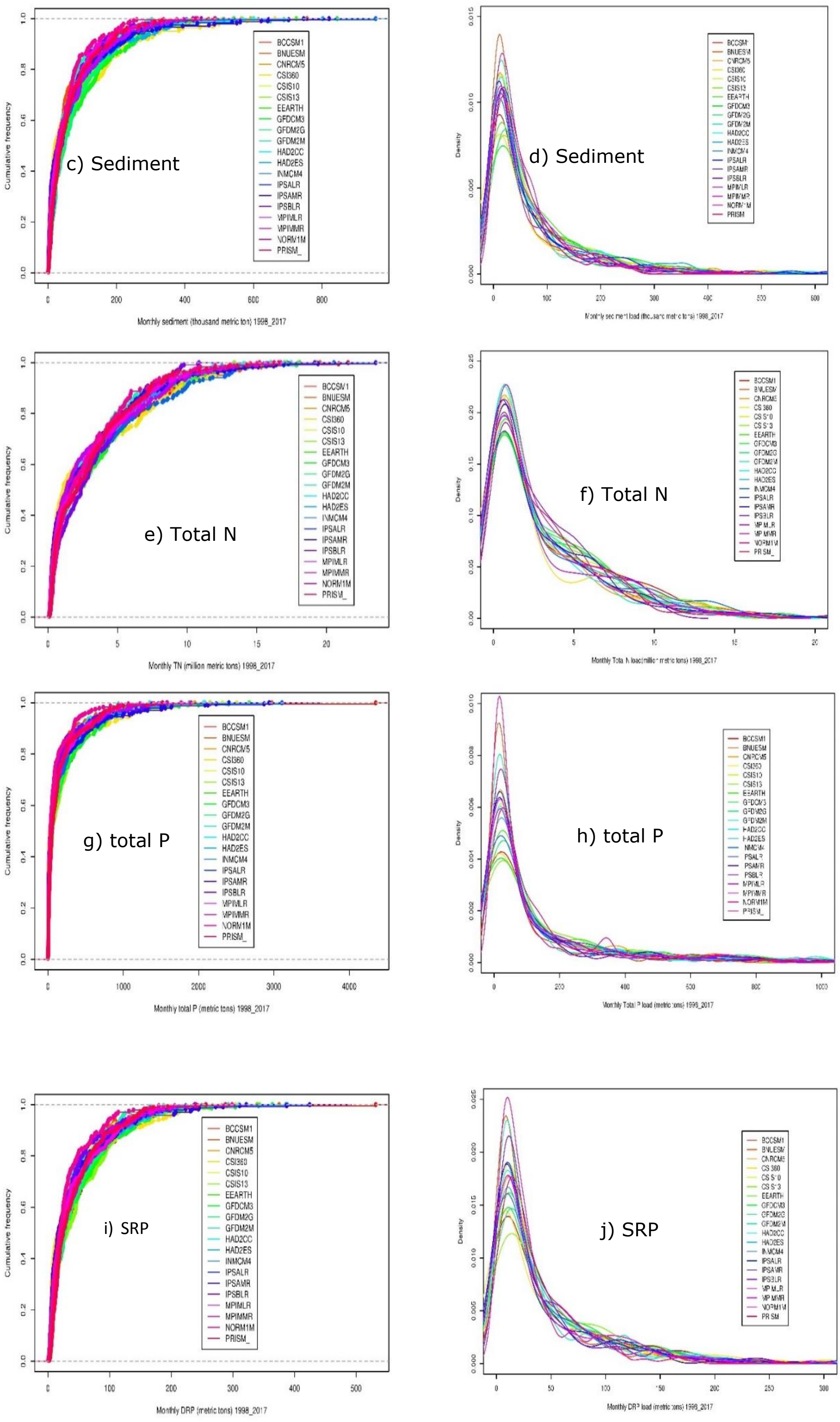
c) Sediment
Cumulative frequency
Monthly sediment (thousand metric ton) 1998_2017
BCCSM1
BNUESM
CNRCM5
CSI360
CSIS10
CSIS13
EEARTH
GFDCM3
GFDM2G
GFDM2M
HAD2CC
HAD2ES
INMCM4
IPSALR
IPSAMR
IPSBLR
MPIMLR
MPIMMR
NORM1M
PRISM_
d) Sediment
Density
e) Total N
Monthly TN (million metric tons) 1998_2017
f) Total N
g) total P
Monthly total P (metric tons) 1998_2017
h) total P
i) SRP
Monthly DRP (metric tons) 1998_2017
j) SRP

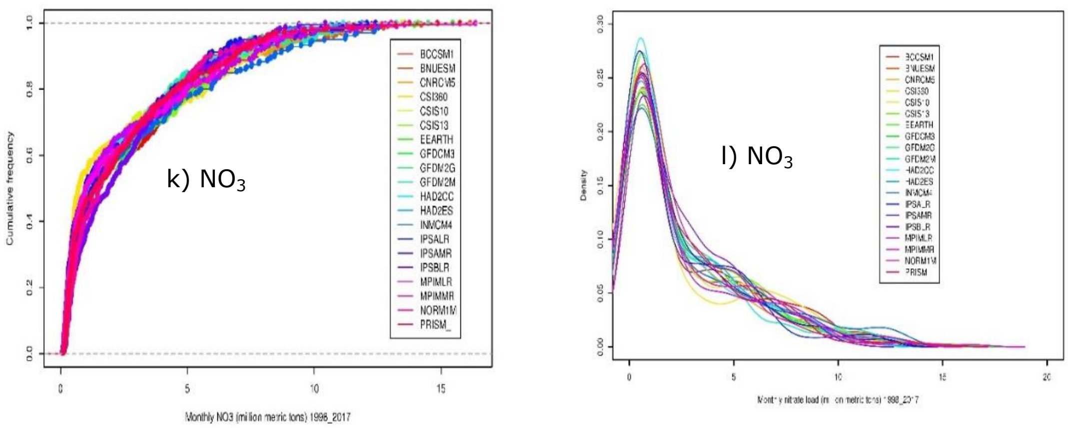

Figure 11. Cumulative density graphs and probability density graphs of monthly mean flow discharge (a and b), and sediment (c and d), total nitrogen (TN) (e and f), total phosphorus (TP) (g and h), soluble reactive phosphorus (SRP) (i and j) and nitrate (NO_3) (k and l) loads for the 19 GCMs and PRISM simulated with SWAT for the USGS Waterville station (N41.5000, W83.7128) from 1998 to 2017.

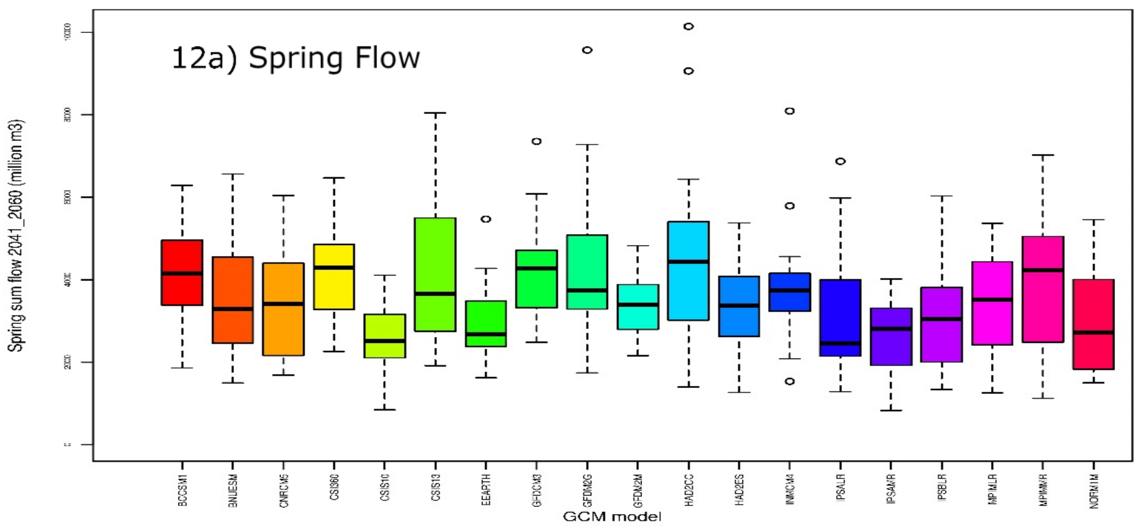

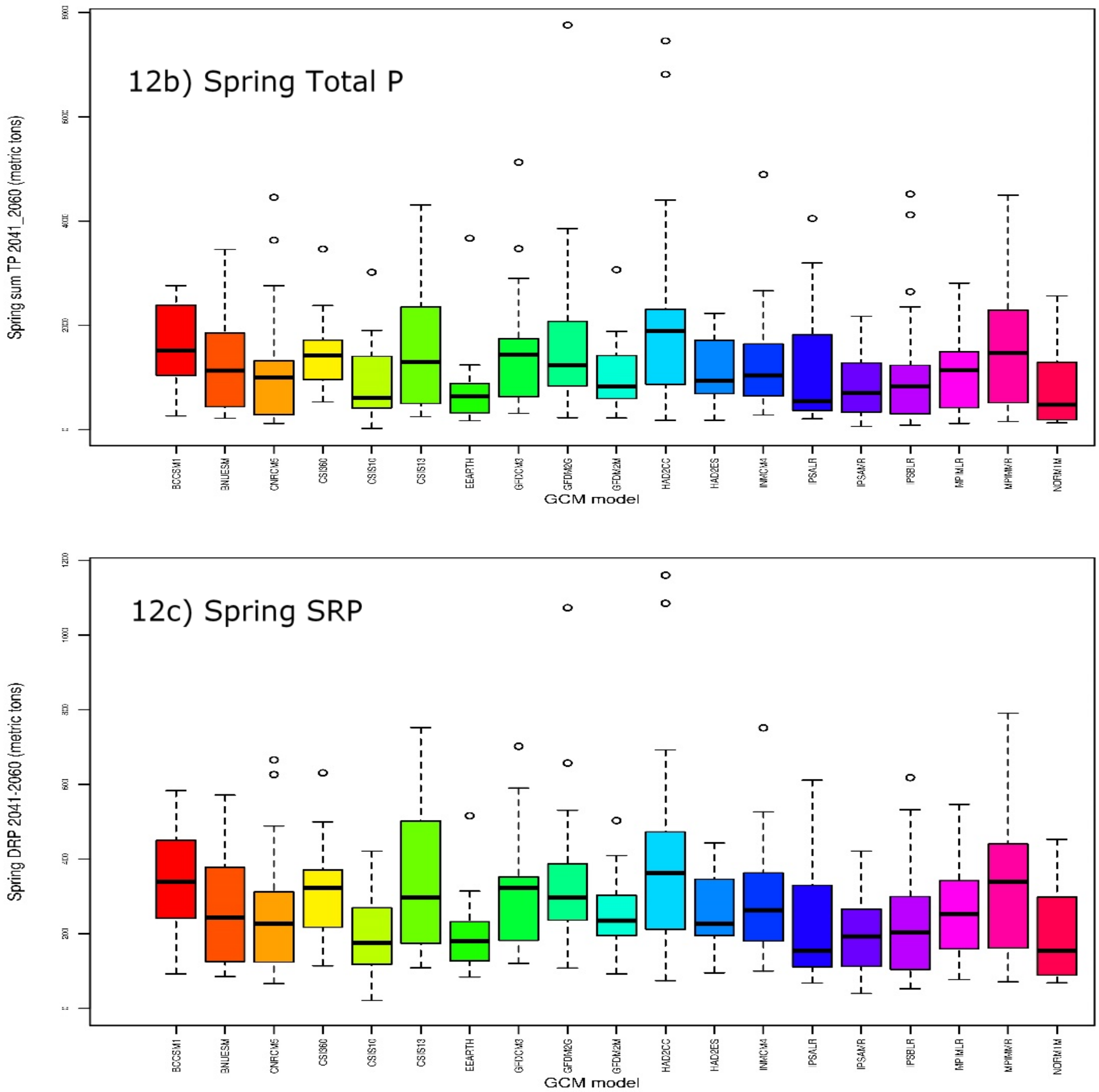

Figure 12. Boxplots of spring total flow volume (a), and TP (b) and SRP (c) loads simulated with SWAT for the 19 GCMs during 2041 and 2060.

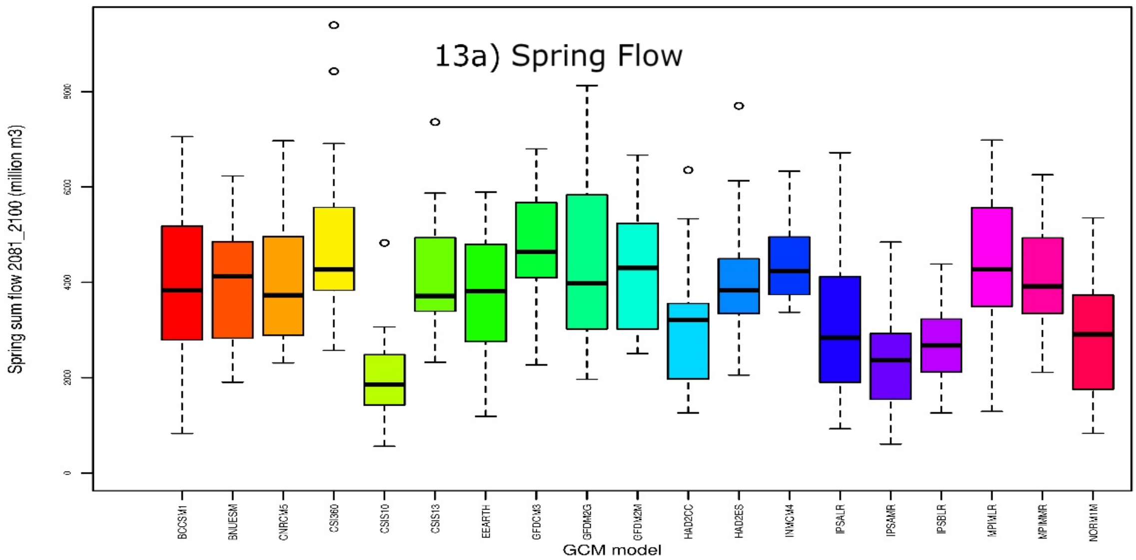

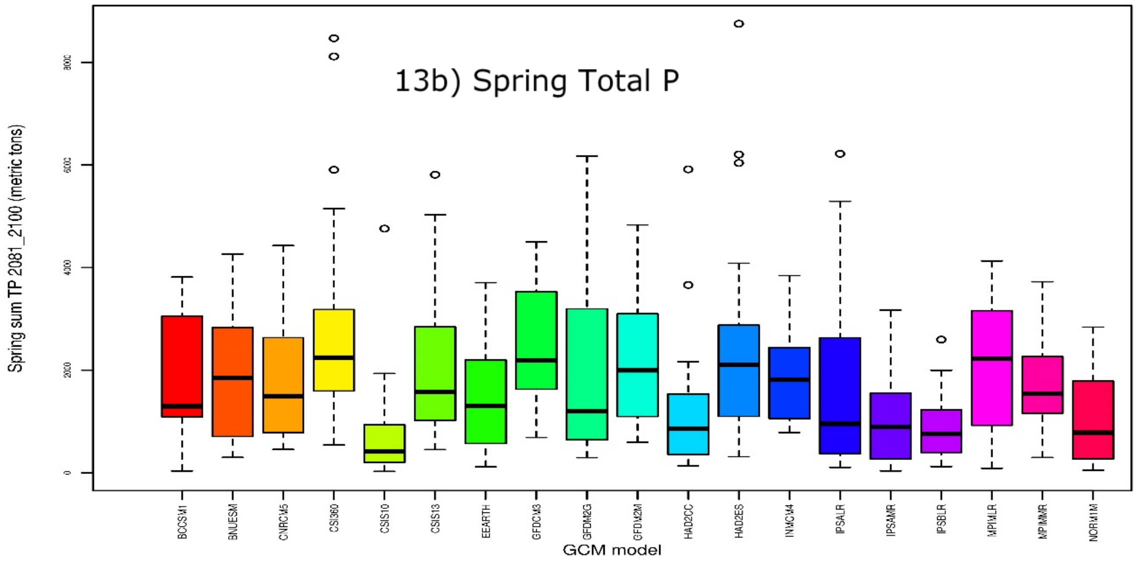

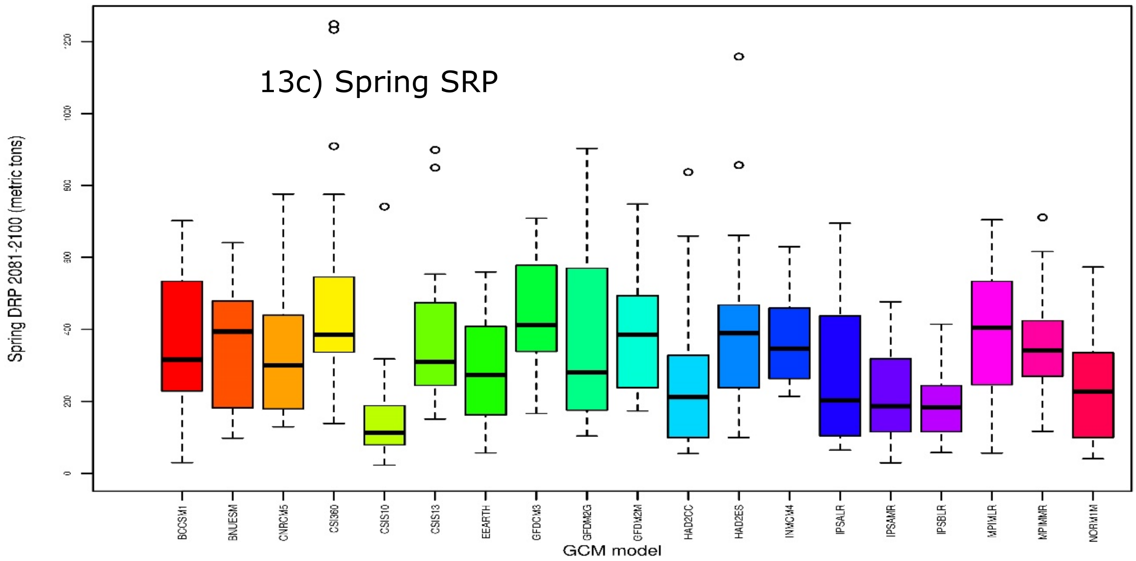

Figure 13. Boxplots of spring a) total flow volume, b) Total P, and c) SRP loads simulated with SWAT for the 19 GCMs from 2081 to 2100.

4.4 Step 4: Algal bloom extent estimation.

Description:

Flow, sediment, nutrient, and climate data were used in the algal bloom model developed by Stumpf et al (2016). Spring (March 1 to July 30) total P and SRP loads (concentration x flow) were used to calculate the bioavailable phosphorus (BioP) using the equation: BioP = (0.26)(total P)(.5) + SRP load. The maximum Cyanobacterial Index (CImax) is then expressed as a function of BioP: CImax= 0.51*10^(2.7/1000*BioP). The Bloom Severity Index (BSI) was then estimated from the CImax using a logarithmic equation: BSI = LOG10(CImax)*7.155141). The BSI were categorized into 5 classes from very mild (BSI < 2) to very severe (BSI > 9). The BSIs were calculated for the historical (2002-2017) and midcentury (2041-2060) periods as well as with and without implementation of conservation practices.

Results:

The occurrence of severe algal bloom is highly uncertain and dependent on so many factors, mainly, flow discharge, nutrients (N&P), temperature, and wind direction and speed. However, very severe blooms occurred with a 12% chance every year during the past 16 years (Figure 13). Several watershed model simulations forced with GCM data revealed that it is likely that the probability of very severe bloom will increase to 24% annually towards 2050 (Figure 13).

The currently recommended suite of conservation practices could reduce the risks of severe algal blooms in the 2050's to 12% probability, similar to the calculated probability for the last 16 years. These management practices, identified at their probable adoption level of based from a survey by Wilson et al (2016) are: 1) targeted new adoption of cover crops to highest total P-loading areas, raising total adoption from the baseline model to 60% of all agricultural lands, 2) targeted adoption of subsurface placement of P fertilizer to highest total P-loading areas, raising total adoption from the baseline model to 68% of all agricultural lands, and 3) targeted adoption of buffer strips to highest total P-loading areas, raising total adoption from the baseline model to 50% of all agricultural area.

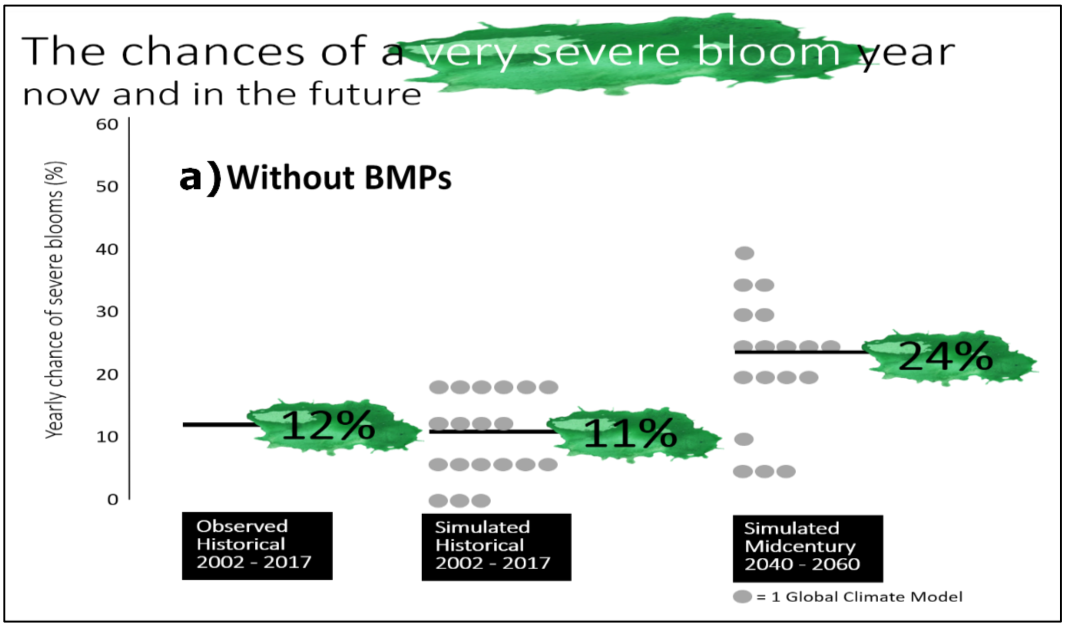

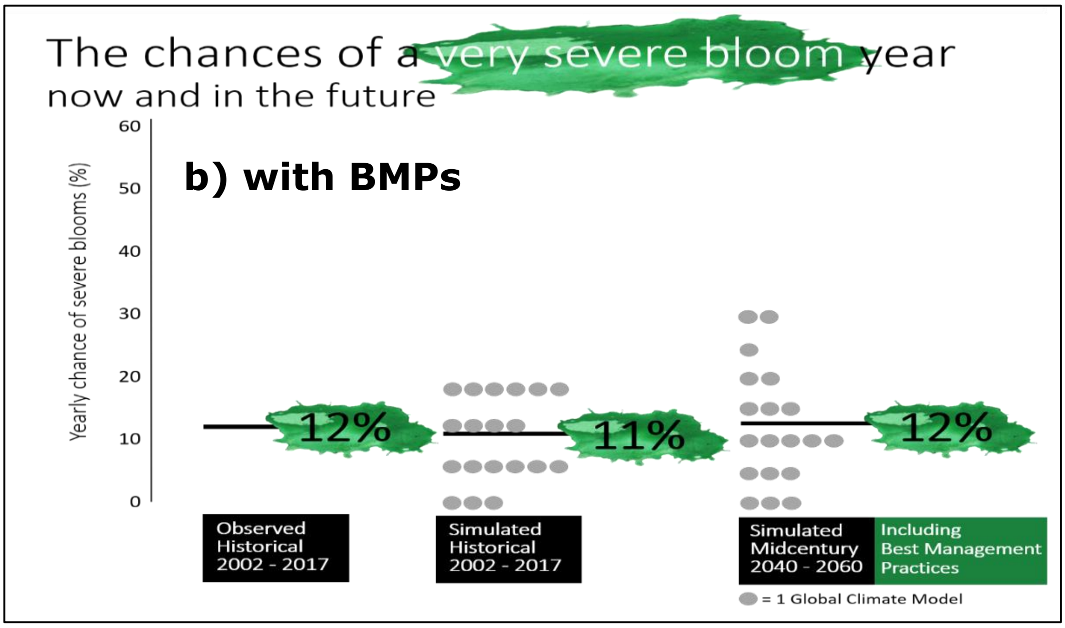

Figure 13. Annual chance of severe blooms in the last 16 years and in the future without (a) and with (b) implementation of BMPs. Each dot represents one climate model and the percentage provides the average of the climate models. (Figures created by Arjen Koekoek and adapted from the NCWQR interactive climate atlas).

4.5 Step 5: Impact assessment and dissemination

Description:

The impact of nutrient and sediment load reduction efficiencies of the landscape management scenarios and at different climate scenarios were evaluated using the local CIIs (e.g. bloom severity index). The combination of "effective" BMPs identified from previous modeling work and their likely adoption rates were tested: 1) 60% acreage implementation of cover crops, 2) 68% acreage subsurface application of P, and 3) 50% acreage adoption of buffer strips (Martin et al., 2016; Prokup et al., 2017).

Results:
Impact model simulation coupled to an algal bloom model showed that without nutrient load reduction practices, the annual severe algal bloom occurrence will increase to 24% probability in the 2050’s. Future implementation of conservation

practices identified from previous impact modeling exercises intended to achieve the 40% load reduction of the 2012 GLWQA, would reduce this risk probability to 12%, similar to the severe algal bloom probability in the last 16 years. Previous trend analyses of historical data showed that the 35% increase in loads is due to increasing flow (precipitation) and the rest due to sources/activities from the agricultural lands (Choquette et al., 2019; Jarvie et al 2017). These findings would explain why the current mitigation will not fully reduce the loading exports: the BMPs are geared towards source reduction but not against the increased precipitation that also increase the flow (and the load exports). Thus, reduction strategies should also focus on practices that modify the hydrologic flow paths and would reduce runoff, tile drain flow, and nutrient exports.

5-Conclusion

The case study objectives were achieved by implementing the specific tasks in each of the five steps of our workflow. Each step was dependent from the previous step. As such, problems and delays in the early steps would create a domino effect as the project progresses. Nonetheless, meticulous data quality assurance and quality control ensured the success of the project.

The Copernicus Climate Change Service (C3S) platform provided downscaled and bias-corrected climate indicators in which the locally-produced climate indicators in the Western Lake Erie Basin were compared and verified with. The platform also offers an easy access to climate change indicators and essential climate variables (ECV's) that could be used to develop and test other mitigation approaches.

We found out that the increased temperature and precipitation would increase the annual occurrence of severe algal blooms to 24% in the 2050's. However, the implementation of best management practices (BMPs) could reduce this risk of annual severe algal blooms occurrence down to the current level of 12%, similar to the past 16 years. Thus, the current mitigation approaches are enough to maintain the risks of severe algal blooms occurrence even with climate change effects in the future. However, "out-of-the-box" mitigations is necessary to further reduce the risks of severe algal bloom occurrence lower than the current levels and reduce the nutrient loads to achieve one of the goals of the 2012 Great Lakes Water Quality Agreement (GLWQA) in the future.

The information from this project could provide guidance on load reduction policies and could help develop contingency management plans in anticipation of the climate change effects on water quality and quantity at Lake Erie, particularly in algal bloom mitigations.

References

Burr, W. S., Takahara, G., & Shin, H. H. (2015). Bias correction in estimation of public health risk attributable to short-term air pollution exposure. Environmetrics, 26(4), 298-311.

Choquette, A.F., Hirsch R.M., Murphy J.C., Johnson L.T., Confesor Jr., R. B. (2019). Tracking changes in nutrient delivery to western Lake Erie: Approaches to compensate for variability and trends in streamflow. Journal of Great Lakes Research (in Press).

Daly, C., Neilson, R. P., & Phillips, D. L. (1994). A statistical-topographic model for mapping climatological precipitation over mountainous terrain. Journal of applied meteorology, 33(2), 140-158.

Flint, L. E., & Flint, A. L. (2012). Downscaling future climate scenarios to fine scales for hydrologic and ecological modeling and analysis. Ecological Processes, 1(1), 2.

Hastie, T. J. (1992). Generalized additive models. Chapter 7 of Statistical Models in S. eds J. M. Chambers and T. J. Hastie, Wadsworth & Brooks/Cole.

Jarvie, H. P., Johnson, L. T., Sharpley, A. N., Smith, D. R., Baker, D. B., Bruulsema, T. W., & Confesor, R. (2017). Increased soluble phosphorus loads to Lake Erie: Unintended consequences of conservation practices? Journal of environmental quality, 46(1), 123-132.

Martin, J.; Aloysius, N.; Howard, G.; Kalcic, M. M.; Wilson, R. S.; Scavia, D.; Roe, B. Reducing Lake Erie's Harmful Algal Blooms: Projection and Adoption of Management Plans. American Geophysical Union, Fall Meeting 2016, abstract #H11F-02.

Prokup, A., R.Wilson, C.Zubko, A.Heeren, and B. Roe. 2017. 4R Nutrient Stewardship in the Western. Lake Erie Basin. Columbus, OH: The Ohio State University, School of Environment & Natural Resources. (https://4rcertified.org/wp-content/uploads/2017/02/Prokup.etal_.2017.4R-Nutrient-Stewardship-in-the-western-Lake-Erie-basin.pdf)

Scavia D, M Kalcic, R L Muenich, J Read, N Aloysius, J Arnold, C Boles, R Confesor, M Gildow, JMartin, T Redder, S Sowa, H Yen. (2017). Multiple models guide strategies for agricultural nutrient reductions. Frontiers in Ecology and the Environment, 15(3), 126-132.

Stumpf, R. P., Johnson, L. T., Wynne, T. T., & Baker, D. B. (2016). Forecasting annual cyanobacterial bloom biomass to inform management decisions in Lake Erie. Journal of Great Lakes Research, 42(6), 1174-1183.

Wolberg, G., & Alfy, I. (2002). An energy-minimization framework for monotonic cubic spline interpolation. Journal of Computational and Applied Mathematics, 143(2), 145-188.

Yin, Y., Jiang, S., Pers, C., Yang, X., Liu, Q., Yuan, J., ... & Zheng, Z. (2016). Assessment of the spatial and temporal variations of water quality for agricultural lands with crop rotation in China by using a HYPE Model. International journal of environmental research and public health, 13(3), 336.